PHYSICAL REVIEW B VOLUME 41, NUMBER 14 15 MAY 1990-I

Relocation of Si atoms in kilo-electron-volt and mega-electron-volt Si-ion irradiation of crystalline Si

J. Keinonen, M. Hautala, I. Koponen, and M. Erola
Accelerator Laboratory, University of Helsinki, Hämeentie 100, SF-00550 Helsinki 55, Finland
(Received 17 January 1990)

Ion-beam mixing of tracer ^{30}Si impurity in crystalline Si sample, irradiated with 2.0×10^{16} 100-keV and 2.0×10^{17} 4-MeV ^{28}Si/cm^2 at room temperature, has been investigated in order to obtain knowledge about the displacement processes in ion bombardment of Si. The tracer ^{30}Si impurity was deposited by implanting a fluence of 1×10^{16} 10-keV ^{30}Si/cm^2 into Si(100) substrates. The mixing of the collisionally similar and chemically identical atoms was studied with the nuclear-resonance-broadening technique. In the simulation of the experimental data, the collisional mixing was described with a new computational method and analytical calculation. The results suggest that the collisional mixing is a dominant contribution to displacement processes in room-temperature ion bombardment of crystalline Si.

I. INTRODUCTION

Ion implantation of crystalline silicon (*c*-Si) is a basic technique in semiconductor technology. In ion-beam modifications of *c*-Si, a fundamental knowledge of the displacement processes in collision cascades is desirable. Processes that generate damage in *c*-Si during the implantation of keV and MeV ions have been studies extensively, e.g., Refs. 1–7, and references therein. Due to several implantation variables (temperature, flux, fluence, ion mass, and energy), there is still some controversy about importance of different processes. Quantitative analysis of ion-beam-mixing experiments can also be utilized to obtain information on basic processes in displacement cascades produced by the slowing down of energetic ions.[8,9] Concerning underlying mechanisms, the ion-beam-mixing studies reported for both silicide-forming elements and fully miscible element Ge are subject to considerable ambiguities since so many physical effects have been found to contribute to ion-beam mixing.[10]

Initially, ion-beam mixing of layered solid systems has been thought to be due to energetic collisional processes.[11–15] The amount of measured mixing has been characterized by the mixing efficiency that is proportional to the spread of a marker or interface of a bilayer during ion-beam bombardment.[10] Mixing efficiency has been observed to correlate with thermodynamical or chemical properties of the substrate and mixing materials.[10] In experiments done with bilayers, correlation with the heat of mixing has been seen.[16,17] In recent marker measurements, the mixing efficiency has been observed to correlate with the cohesive energy and tracer impurity diffusion.[18–20] The measured mixing efficiency has in many cases been claimed to be an order of magnitude higher than predicted by collisional models.[18,19] These observations have been interpreted to indicate that collisional mixing is a secondary contribution at low temperatures and that the diffusion within the thermal spike is the most important contribution to ion-beam mixing.[10,19,21,22] This conclusion is, however, not unambiguous.

The estimates of collisional mixing have been based on the results of theoretical calculations that include approximations whose validity is questionable.[11,13,15] Computer simulations have recently given indication that collisional mixing may be larger than expected on the basis of the earlier theoretical estimates.[23,24] It has been claimed that theory with more realistic parameters would give results comparable with computer simulations.[25] Furthermore, collisional mixing may well be dominated by low-energy collisions that are sensitive to interaction potential in the electron-volt region. The reduced vacancy-migration enthalpy in a thermal-spike phase[26] confuses also a direct comparison of the mixing efficiencies with the chemical properties of a target. Recent calculations with a new two-step computational method further support a more important contribution of the collisional mixing than taken into account previously.[27]

The present work was undertaken to investigate the relocation of matrix atoms in collisional processes. Information about the displacement was obtained in experiments carried out by using a thin tracer ^{30}Si impurity layer implanted into *c*-Si and irradiated with ^{28}Si ions at room temperature. In ^{28}Si-ion irradiations, no chemically different impurities were introduced into the samples and no impurity atoms were included in collisional cascades. Effects due to different spatial structures of collision cascades were studied by the use of the 100-keV and 4-MeV irradiation energies. Since only Si atoms were present, the stopping conditions remained constant during the irradiations. Therefore, the cumulative mixing could be calculated accurately. Predominant vacancy defects in *c*-Si ion implanted at room temperature, have been shown to be divacancies.[5,28–30] Based on this observation and the migration of vacancies at room temperature,[31] the relaxation of the highly nonequilibrium state following the displacement process includes the effects of vacancy migration into the bulk.

 ©1990 The American Physical Society

II. EXPERIMENTAL PROCEDURE AND RESULTS

The samples were prepared at the isotope separator of the laboratory by implanting a fluence of 1×10^{16} 10-keV ^{30}Si/cm^2 into n-type Si(100) slices (Czochralski grown, doped uniformly by P to a resistivity of 2.5–3.5 Ω cm) at room temperature. The irradiations were carried out at room temperature, with electrostatically scanned (over a 9-mm-diameter area) 100-keV (1.3 μA) ^{28}Si$^+$ beam from the isotope separator and 4-MeV (400 particle nA) ^{28}Si^{2+} beam from the 5-MV tandem accelerator EGP-10-II of the laboratory. The heating of the samples during the irradiations was avoided by the use of the low beam powers. During the implantations and irradiations, the specimen normal (⟨100⟩ axis) was aligned 6° from the beam axis.

To probe the ^{30}Si concentration distributions in the samples, the nuclear-resonance-broadening (NRB) technique was used.[32] The use of the sharp ($\Gamma=68$ eV, Ref. 33), strong ($S=5$ eV, Ref. 33), and isolated resonance of the ^{30}Si(p,γ)^{31}P reaction at $E_p=620$ keV made it possible to profile ^{30}Si distributions with a good depth resolution. The proton beams of about 1 μA were supplied by the 2.5-MV Van de Graaff accelerator of the laboratory. The resolving power of the beam, typically 400 eV, corresponded to the depth resolution of about 5 nm at the surface. The beam was focused to a spot of 3×3 mm^2. Effects associated with the probing proton beam were controlled by repeating the measurement of each distribution two times at each beam spot. By attaching a target with clamps to a copper plate kept at room temperature, no effects were observed. The γ radiation was detected in a 12.7-cm-diameter×10.2-cm NaI(Tl) crystal shielded against the background radiation by 5 cm of lead.

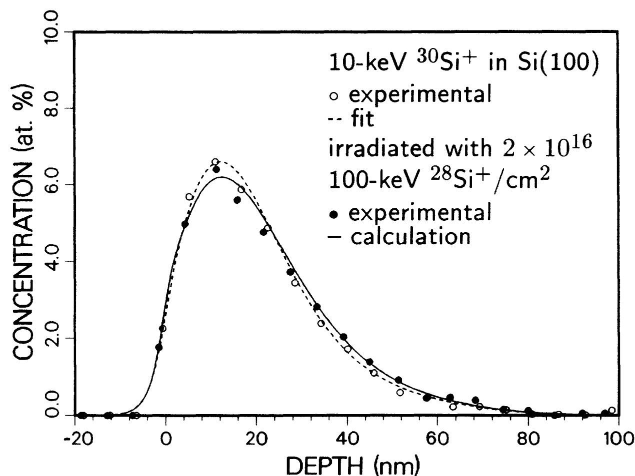

FIG. 1. Measured ^{30}Si distribution corresponding to a virgin region (open circles) and to a region irradiated with 2.0×10^{16} 100-keV ^{28}Si/cm^2 (solid circles). The computer simulations of the mass distributions after the irradiation are shown by the solid line. A possible sputtering (less than 2 nm, see the text) is not taken into account in the location of the simulated mass distribution. The mass distribution used in the computer simulations for the virgin sample is shown by the dashed line.

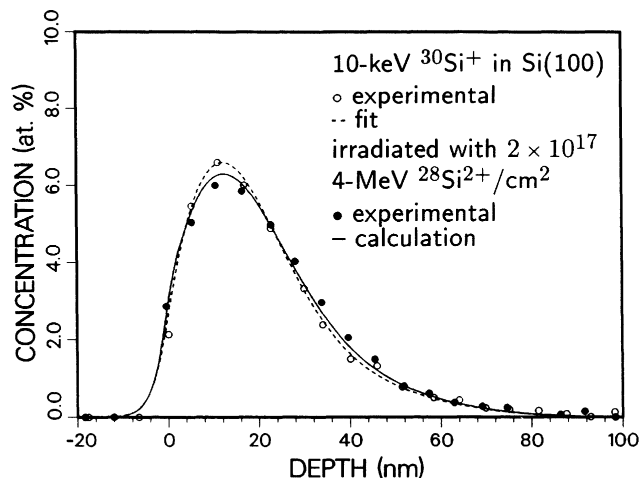

FIG. 2. Measured ^{30}Si distributions corresponding to a virgin region (open circles) and to a region irradiated with 2.0×10^{17} 4-MeV ^{28}Si/cm^2 (solid circles). The computer simulations of the mass distributions after the irradiation are shown by the solid line. The mass distribution used in the computer simulations for the virgin sample is shown by the dashed line.

The measured ^{30}Si distributions corresponding to a virgin region and to a region irradiated with 2.0×10^{16} 100-keV ^{28}Si/cm^2 are shown in Fig. 1 and those corresponding to a virgin region and to a region irradiated with 2.0×10^{17} 4-MeV ^{28}Si/cm^2 in Fig. 2. The width is contributed to by the range distribution of 10-keV ^{30}Si implants, the natural width of the resonance, the energy resolution of the proton beam, and the width of the energy-loss distribution for protons after traversing in Si. In the nuclear-resonance-broadening (NRB) measurements of the samples, the concentration profiles of doped ^{30}Si atoms were obtained by comparison of the γ-ray yields from the doped ^{30}Si nuclei with those from isotope ^{30}Si in natural silicon (3.1 at. %). In the calculation of the depth scale,[32] the stopping power of silicon for protons was taken from Ref. 34. The areas of the distributions illustrated in Figs. 1 and 2, indicated that the amounts of sputtered Si atoms due to the ^{28}Si bombardments were negligible. Because of low abundance (3.1 at. %) of the isotope ^{30}Si in natural silicon, low concentrations of implanted ^{30}Si could be measured reliably. The fluences were measured by integrating ion current collected on a target equipped with a suppression for secondary electrons. The irradiation fluences Φ were selected so that the same total deposited energy $\Phi F_D=5\times10^{17}$ eV/Å in the region of the implanted ^{30}Si atoms was obtained in the 4-MeV and 100-keV irradiation. F_D is the energy (eV) per ion deposited in nuclear collisions in the lattice per unit depth (Å). The numerical values were obtained in collision cascade calculations, see below.

In order to accurately know the deposited energy distribution in the 100-keV irradiation, the range distributions of 10-, 50-, and 100-keV ^{30}Si ions in c-Si were measured and simulated by computer calculations. The measured and computer simulated (see below) profiles are

shown in Fig. 3. The samples were prepared by implanting the fluences of 1×10^{16} 10-keV, 2×10^{16} 50-keV, and 1×10^{17} 100-keV $^{30}Si^{+}/cm^{2}$ into Si(100) specimen, whose normal was aligned 6° from the axis.

In order to study the relaxation of *c*-Si during the Si irradiation, a Si(100) sample implanted by 3-keV protons in an ultrahigh-vacuum chamber (the vacuum about 0.1 μPa) at room temperature to a fluence of 1×10^{16} protons/cm^2 was also prepared. In the room-temperature implantation, the *c*-Si sample was recovered from the proton-induced damage that would affect the results of Si irradiation at or below the room temperature. The reason behind the use of the 3-keV-proton-implanted sample, was the sensitivity of hydrogen migration to defects in *c*-Si.[5,7] The sample was irradiated by 4-MeV $^{28}Si^{2+}$ ions to a fluence of 2.0×10^{17} Si/cm^2 at 12 K. The depth profilings of H by the NRB technique were carried out at 12 K and consequently at room temperature at the tandem accelerator EGP-10-II of the laboratory, using an about 100-nA $^{15}N^{2+}$ beam in conjunction with the 6.385-MeV resonance in the reaction $^{1}H(^{15}N,\alpha\gamma)^{12}C$.[35] The H distributions are illustrated in Fig. 4.

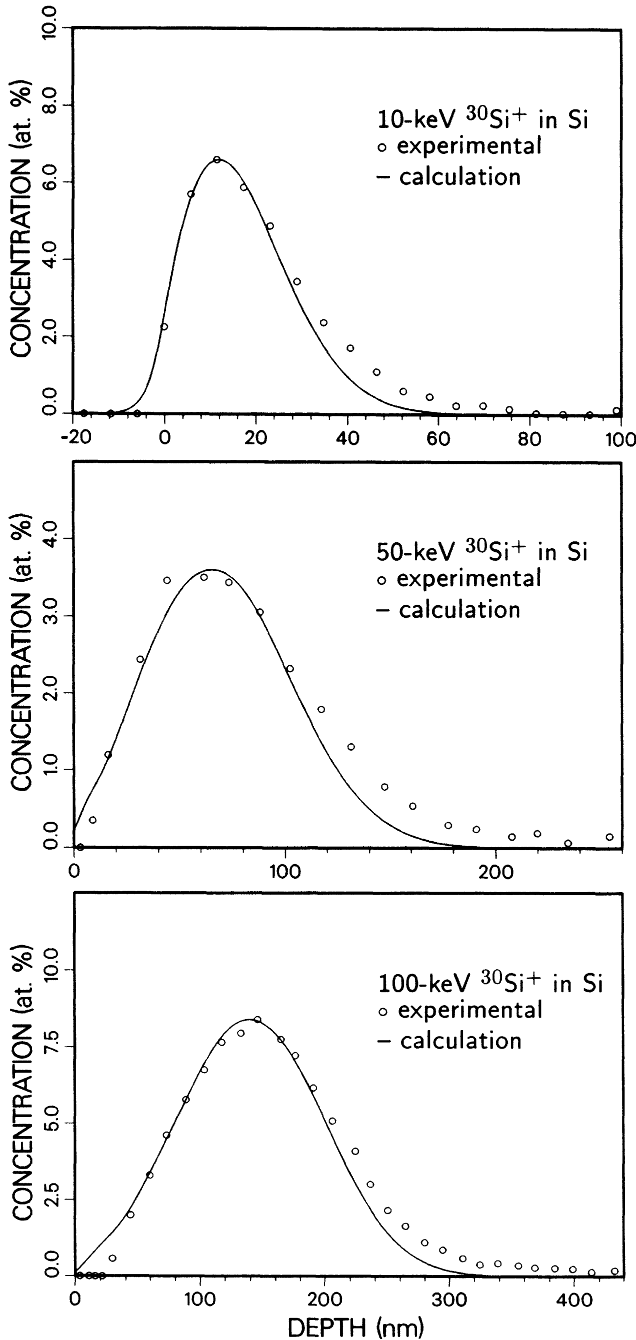

FIG. 3. Range distributions of 10-, 50-, and 100-keV ^{30}Si ions. The measured distributions are compared with mass distributions obtained from Monte Carlo simulations.

In the irradiation of the sample at 12 K, which is below the temperature of monovacancy migration (150 K, Ref. 31), the monovacancies were accumulated in the collision-cascade region of the sample. Release of these defects by rising the temperature to the room temperature lead to a strong relaxation of the lattice and to a loss of H from the implanted region, Fig. 4. In a room-temperature irradiation with the 4-MeV $^{28}Si^{2+}$ ions, no change in the H profile was observed. This demonstrates the importance of the monovacancy migration for the lattice relaxation after each collisional cascade during irradiations at room temperature.

III. COMPUTER SIMULATIONS

A. ^{30}Si distributions

For the comparisons of the simulated mass distributions of ^{30}Si with the measured distributions (Figs. 1–3), the calculated mass profiles were convoluted with the natural width of the resonance, the energy resolution of the proton beam, and the width of the energy-loss distribution for protons after traversing in Si. The width of

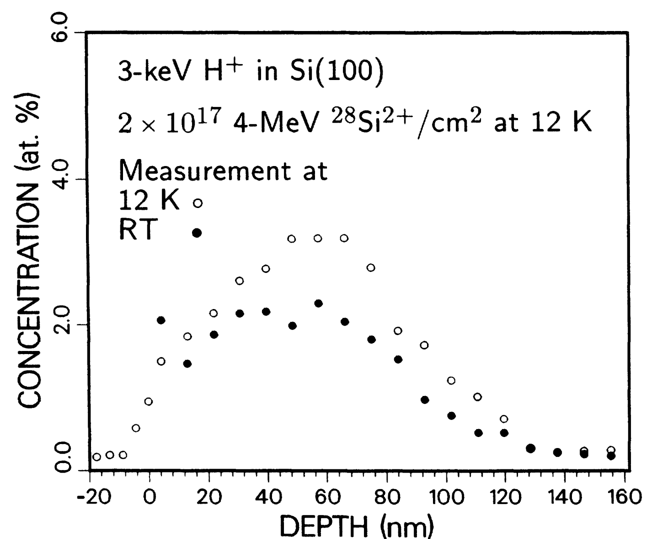

FIG. 4. Hydrogen distributions of the 1×10^{16} 3-keV protons/cm^2 in *c*-Si irradiated by 4-MeV ^{28}Si ions at 12 K to a fluence of 2.0×10^{17} Si/cm^2 and measured at 12 K and consequently at room temperature.

the energy loss distribution for protons will be considered in the following, since it was determined in the present work.

In the numerical convolution we used a function $f(z)$, which approximates well Vavilov's energy straggling distribution[36] at depth x

$$f(z)=\frac{1}{(2\pi\Omega^2)^{1/2}}\exp\left[-\frac{S^2(x-z)^2}{2\Omega^2}\right], \quad (1)$$

where S is the stopping power for protons[34] and Ω^2 is the energy straggling at depth x. Near the surface, the best agreement between the simulated and experimental range distributions was obtained when the energy straggling Ω^2 calculated according to the Lindhard-Scharff model[37] was multiplied by 0.5.

Excluding the tails of the experimental 10-, 50-, and 100-keV range profiles, the simulated ^{30}Si distributions are in a good agreement with the measured distributions. The reason for the tail is ^{30}Si atoms channeled during the slowing-down process in *c*-Si. In the Monte Carlo simulations[38,39] of the range profiles, the Si sample was assumed to be amorphous. The stopping power used for Si ions will be discussed in the connection of the mixing.

B. Collisional mixing, a two-step method

Conventionally, the amount of measured mixing has been characterized by the spread of a marker or interface of a bilayer during ion irradiation. In the present geometry, the displacement of tracer ^{30}Si atoms had to be studied in the whole region of the implanted concentration distribution.

The two-step method used in this work to simulate the measured mixing is explained in Ref. 27. If the initial position of an atom within the 10-keV range distribution is x from the surface, the Monte Carlo simulation[38,39] is very well suited to calculate the differential cross section $d\sigma(x,z)$ for the scattering process that causes the atom to relocate from x to $(x+z, x+z+dz)$ due to a single-ion collision. The calculated relocation cross sections per relocation depth unit dz at $x=15$ nm are shown in Fig. 5 for 100-keV and 4-MeV ^{28}Si irradiations. The depth 15 nm corresponds to the modal range of 10-keV ^{30}Si ions in *c*-Si.

The recoil cross sections were based on a mean potential,[38] where the interaction potential is assumed to be a screened Coulomb potential with a Thomas-Fermi screening length. The screening function was obtained by fitting a polynomial consisting of a sum of exponentials to 50 ion-atom potentials obtained using Dirac-Fock calculations of the electron densities.[38] This mean potential is close to the so-called Ziegler-Biersack-Littmark potential.[40,41] The electronic energy loss was described by a frictional force from the Lindhard-Scharff-Schiøtt theory.[42] The recoils in a cascade were followed until their energy fell below 4 eV.

The relocation of atoms during an ion bombardment to a fluence Φ was calculated by describing the movement of an atom as a random-walk process with various step lengths of different probabilities obtained from the Poisson distribution. Repeated to a large number of impurity atoms, this yields a relocation profile of a thin tracer marker.

For a comparison with an experimental concentration profile, calculated relocation profiles of thin markers were convoluted with the mass distribution of implanted 10-keV ^{30}Si atoms. As shown in Fig. 3, the calculated range distribution does not include channeled atoms. For an accurate comparison with the experimental profiles after the ^{28}Si irradiations, a mass profile was searched that yielded an identical range distribution with the experimental one shown in Fig. 3. This mass profile was then convoluted with the relocation profile of a thin marker and the straggling of the proton energy loss, Eq. (1). The final computer-simulated distributions are compared with the experimental ones in Figs. 1 and 2.

Sputtering of the sample surface due to the 2.0×10^{17} 4-MeV Si bombardment should be negligible, whereas the 2.0×10^{16} 100-keV Si bombardment could yield some erosion of the surface. Since the corresponding sputtering coefficients have not been measured,[43] the sputtering yield reported for 100-keV Ne^+ ions incident on Si was used to estimate an upper limit of 2 nm for the erosion of Si surface in the irradiation with 2.0×10^{16} 100-keV $^{28}Si/cm^2$. The corresponding loss of implanted ^{30}Si atoms is so low that it could not be obtained experimentally. No correction for sputtering was done for the simulated concentration distribution. On the basis of the reported sputtering yield curve for Ne^+ ions,[43] the sputtering in the 2.0×10^{17} 4-MeV Si bombardment is negligible.

C. Collisional mixing, an analytical analysis

In the present case the cumulative effect of the successive relocations can also be calculated analytically. In an isotropic cascade mixing,[13] the relocation cross sections are predicted to be symmetric. Excluding the small asymmetry, this condition is fulfilled by the calculated re-

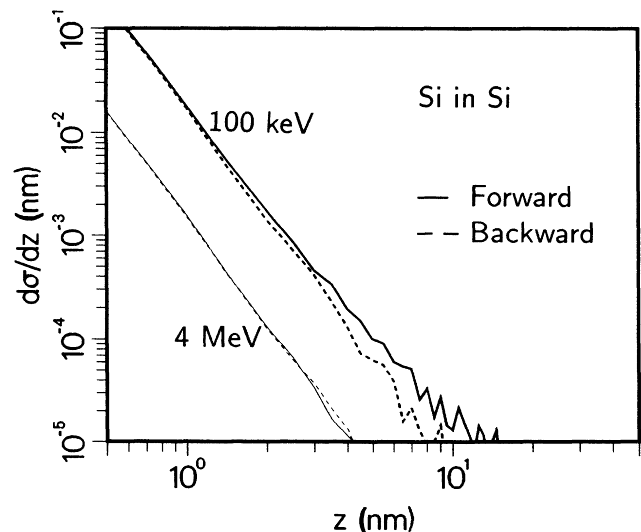

FIG. 5. Relocation cross sections per relocation depth unit at the depth of 15 nm, which corresponds to the modal range of 10-keV ^{30}Si ions in *c*-Si.

location cross sections $d\sigma(x,z)$ as illustrated in Fig. 5. The cross sections can be described by the power-law equation

$$d\sigma(x,z)=\Gamma\frac{F_D(x)}{N}\frac{1}{2(\alpha+1)}\left[\frac{|z|}{A}\right]^{-1-1/\alpha}d\left[\frac{z}{A}\right], \quad (2)$$

where N is a particle density, A, α, and Γ are well-defined constants[13] and $F_D(x)$ is deposited energy per unit depth. The cross section depends only slightly on x through $F_D(x)$.

Adopting the so-called diffusion approximation,[12] relocation profile $P(x,z)$ for a marker is easily shown to be

$$P(x,z)=\frac{1}{[2\pi\sigma^2(x)]^{1/2}}\exp\{-[z-m(x)]^2/[2\sigma^2(x)]\}, \quad (3)$$

where

$$m(x)=\Phi\int_z z\,d\sigma(x,z) \quad (4)$$

and

$$\sigma^2(x)=\Phi\int_z z^2\,d\sigma(x,z) \quad (5)$$

are the first and second moment of the relocation cross section, respectively, for a fluence Φ. For nearly symmetric relocation cross sections, the moments $m(x)$ and $\sigma^2(x)$ can be expressed in terms of corresponding moments at the depth x_0, which was chosen to be 15 nm, i.e., the modal range of 10-keV ^{30}Si ions in *c*-Si;

$$m(x)=\frac{F_D(x)}{F_D(x_0)}m_0 \quad (6)$$

$$\sigma^2(x)=\frac{F_D(x)}{F_D(x_0)}\sigma_0^2 . \quad (7)$$

Note that the moments are proportional to the deposited energy $F_D(x)$. This is a consequence of the relocation cross section given in Eq. (2).

Once the relocation profile $P(x,z)$ is known, the mixed concentration distribution is calculated by convoluting the initial concentration distribution $c_0(x)$ with $P(x,z)$ (Ref. 12)

$$c(x)=\int_{x'}P(x,x-x')c_0(x')dx' . \quad (8)$$

By the use of Eqs. (3) and (8) the matrix relocation is omitted. For the inclusion of the effect, the analysis should be done by means of balance equations.[12,14,15] However, because of the relatively low tracer atom concentration and the fact that the tracer ^{30}Si atoms do not change the stopping conditions, the effect of the matrix relocation is small and was estimated in the following way.[13] The change of the depth scale $x\rightarrow x+\delta z(x)$ was calculated assuming that macroscopic density gradient $\delta N(x)$ due to matrix relocation relaxes. If the deposited energy is a slowly varying function of x, the change of the depth scale is given by the following equation:

$$\delta z(x)=-m(x)+\sigma^2(x)\frac{d}{dx}[\ln F_D(x)] . \quad (9)$$

In the studied cases only the first term is significantly different from zero in the region of interest. Then $\delta z(x)$ cancels the peak shift $m(x)$ given in Eq. (4).

The calculated results agree completely with profiles simulated with the two-step method. The sputtering (see above) and its effect on the relocation cross section were not taken into account in the calculations.

IV. DISCUSSION

In the Si-ion irradiations of the ^{30}Si-implanted *c*-Si, the spike and long-range transport effects are reduced in the relocations of Si atoms due to the similar and light atomic masses. In the region of collisional cascades where all the atoms are chemically identical, chemical driving forces (e.g., heat of mixing) have no effect on the mixing. It is most likely that diffusional mixing due to defect migration plays a role during the mixing process. A correlation with cohesive energy could be a way to try to explain the observed mixing as a radiation-enhanced diffusion process.[16] However, the agreement between the experimental results obtained in the 100-keV and 4-MeV ^{28}Si-ion irradiations to fluences of 2.0×10^6 and 2.0×10^{17} ions/cm^2 cannot be explained in accordance with the model presented in Ref. 16. On the other hand, the agreement between the measured and simulated profiles indicates that the collisional mixing dominates the relocation of Si atoms. The movement of ^{30}Si atoms was assumed to be due to knock on by the projectiles (recoil implantation) and recoiling target atoms (cascade mixing). By the use of the keV and MeV energies, the spatial structures of collision cascades were different. The agreement between the experimental results and between the calculated and experimental results shows that the relocation of Si atoms depends predominantly on several low-energy two-body collisions during the ballistic phase.

If the matrix relocation does not broaden the ^{30}Si distribution but results only in its shift as assumed above, all the ballistic processes were included in the calculations. In fact the numerical solution of the balance equations[12,14,15] describing the mixing and matrix relocation does not either yield an additional broadening of the ^{30}Si distribution due to the matrix relocations. Phenomena related to vacancy and atom migration, such as the matrix relaxation through the migration of vacancies and migration during the cooling period of the cascades, were neglected in the calculations.

In our earlier studies, mixing of Al marker in *c*-Si irradiated with Ne ions[8] or Al bilayer on *c*-Si irradiated with Ar ions[9] was obtained to be 3–7 times larger than expected according to the conventional estimate for the ballistic mixing. The reanalysis of those experimental results with the present calculations shows that the mixing of Al atoms in *c*-Si is dominated by the collisional process.

In conclusion, we have shown that in Si-ion irradiation of *c*-Si at room temperature, relocation of Si atoms is dominated by the collisional process.

ACKNOWLEDGMENTS

This work was supported by the Academy of Finland.

[1]S. T. Picraux, F. L. Vook, and H. J. Stein, in *Proceedings of the International Conference on Defects and Radiation Effects in Semiconductors, Nice, France, 1978,* edited by J. H. Albany (Institute of Physics, Bristol, England, 1979), p. 31.
[2]W. R. Brown, in *Beam-Solid Interactions and Phase Transformations,* Proceedings of the Materials Research Society, edited by H. Kurz, G. L. Oesan, and J. M. Poate (MRS, Pittsburgh, 1985), Vol. 51, p. 53.
[3]J. S. Williams, in *Beam-Solid Interactions and Phase Transformations,* Ref. 2, p. 83.
[4]W. J. Choyke, R. B. Irwin, J. N. McGruer, J. R. Townsend, K. Q. Xia, N. J. Doyle, B. O. Hall, J. A. Spitznagel, and S. Wood, in *Proceedings of the 13th International Conference on Defects in Semiconductors, Coronade, California 1984,* edited by L. C. Kimerling and J. M. Porsey, Jr. (American Institute of Metallurgical Engineers, Warendale, 1984), p. 789.
[5]J. Keinonen, M. Hautala, E. Rauhala, V. Karttunen, A. Kuronen, J. Räisänen, J. Lahtinen, A. Vehanen, E. Punkka, and P. Hautojärvi, Phys. Rev. B **37**, 8269 (1988).
[6]W. R. Fahrner, J. R. Laschinski, and D. Bräunig, Nucl. Instrum. Methods A **268**, 579 (1988).
[7]J. Mäkinen, E. Punkka, A. Vehanen, P. Hautojärvi, J. Keinonen, M. Hautala, and E. Rauhala, J. Appl. Phys. (to be published).
[8]H. J. Whitlow, J. Keinonen, and M. Hautala, J. Appl. Phys. **58**, 3246 (1985).
[9]M. Erola, J. Keinonen, M. Hautala, and M. Uhrmacher, Nucl. Instrum. Methods Phys. Res. Sect. B **34**, 42 (1988).
[10]B. M. Paine and R. S. Averback, Nucl. Instrum. Methods Phys. Res. Sect. B **7/8**, 666 (1985).
[11]H. H. Andersen, Appl. Phys. **18**, 131 (1979).
[12]A. Gras-Marti and P. Sigmund, Nucl. Instrum. Methods **180**, 211 (1981).
[13]P. Sigmund and A. Gras-Marti, Nucl. Instrum. Methods **182/183**, 25 (1981).
[14]U. Littmark and W. O. Hofer, Nucl. Instrum. Methods **168**, 329 (1980).
[15]U. Littmark, Nucl. Instrum. Methods Phys. Res. Sect. B **7/8**, 684 (1985).
[16]W. L. Johnson, Y.-T. Cheng, M. Van Rossum, and M.-A. Nicolet, Nucl. Instrum. Methods Phys. Res. Sect. B **7/8**, 657 (1985).
[17]R. S. Averback, D. Peak, and L. J. Thompson, Appl. Phys. A **39**, 59 (1986).
[18]S.-J. Kim, M.-A. Nicolet, R. S. Averback, and D. Peak, Appl. Phys. A **41**, 171 (1986).
[19]S.-J. Kim, M.-A. Nicolet, R. S. Averback, and D. Peak, Phys. Rev. B **37**, 38 (1988).
[20]B. V. King, S. G. Puranik, and R. J. Macdonald, Nucl. Instrum. Methods Phys. Res. Sect. B **33**, 657 (1988).
[21]R. S. Averback, Nucl. Instrum. Methods Phys. Res. Sect. B **15**, 675 (1986).
[22]I. A. Fenn-Tye and A. D. Marwick, Nucl. Instrum. Methods Phys. Res. Sect. B **18**, 236 (1987).
[23]W. Möller and W. Eckstein, Nucl. Instrum. Methods Phys. Res. Sect. B **7/8**, 645 (1985).
[24]W. Möller, Nucl. Instrum. Methods Phys. Res. Sect. B **15**, 688 (1986).
[25]K. Johannessen and P. Sigmund, Nucl. Instrum. Methods Phys. Res. Sect. B **19/20**, 85 (1987).
[26]M. W. Guinan and J. H. Kinney, J. Nucl. Mater. **103/104**, 1319 (1981).
[27]M. Hautala and I. Koponen, Nucl. Instrum. Methods Phys. Res. Sect. B (to be published).
[28]H. J. Stein, F. L. Vook, and J. A. Borders, Appl. Phys. Lett. **16**, 106 (1970).
[29]H. J. Stein and W. Beezhold, Appl. Phys. Lett. **17**, 442 (1970).
[30]H. J. Stein, F. L. Vook, D. K. Brice, J. A. Borders, and S. T. Picraux, Radiat. Eff. **6**, 19 (1970).
[31]R. Car, P. J. Kelly, A. Oshiyama, and S. T. Pantelidas, Phys. Rev. Lett. **54**, 360 (1985).
[32]J. Keinonen, J. Räisänen, and A. Anttila, Appl. Phys. A **34**, 49 (1984).
[33]P. M. Endt and C. van der Leun, Nucl. Phys. **A310**, 1 (1978).
[34]H. H. Andersen and J. F. Ziegler, *The Stopping and Ranges of Ions in Matter* (Pergamon, New York, 1977), Vol. 3.
[35]H. J. Whitlow, J. Keinonen, M. Hautala, and A. Hautojärvi, Nucl. Instrum. Methods Phys. Res. Sect. B **5**, 505 (1984).
[36]P. V. Vavilov, Zh. Eksp. Teor. Fiz. **32**, 920 (1957) [Sov. Phys.—JETP **5**, 749 (1957)].
[37]J. Lindhard and M. Scharff, Mat. Fys. Medd. Dan. Vid. Selsk. **27**, No. 15 (1953).
[38]M. Bister, M. Hautala, and M. Jäntti, Radiat. Eff. **42**, 201 (1979).
[39]M. Hautala, Radiat. Eff. **51**, 35 (1980).
[40]J. P. Biersack and W. Eckstein, Appl. Phys. **A34**, 73 (1984).
[41]W. D. Wilson, L. G. Haggmark, and J. P. Biersack, Phys. Rev. B **15**, 2458 (1977).
[42]J. Lindhard, M. Scharff, and H. E. Schiøtt, Mat. Fys. Medd. Dan. Vid. Selsk. **33**, No. 14 (1963).
[43]H. H. Andersen and H. L. Bay, *Topics in Applied Physics, Sputtering by Particle Bombardment I,* edited by R. Behrisch (Springer, Berlin, 1981), Vol. 47, p. 145.